Control of Spinal Motoneurons by Feedback From a Non-invasive Real-Time Interface

Deren Y. Barsakcioglu, *Member, IEEE*, Mario Bräcklein, *Student Member, IEEE*, Aleš Holobar *Member, IEEE,* and Dario Farina, *Fellow, IEEE*

Abstract*— Interfacing with human neural cells during natural tasks provides the means for investigating the working principles of the central nervous system and for developing human-machine interaction technologies. Here we present a computationally efficient non-invasive, real-time interface based on the decoding of the activity of spinal motoneurons from wearable high-density electromyogram (EMG) sensors. We validate this interface by comparing its decoding results with those obtained with invasive EMG sensors and offline decoding, as reference. Moreover, we test the interface in a series of studies involving real-time feedback on the behavior of a relatively large number of decoded motoneurons. The results on accuracy, intuitiveness, and stability of control demonstrate the possibility of establishing a direct non-invasive interface with the human spinal cord without the need for extensive training. Moreover, in a control task, we show that the accuracy in control of the proposed neural interface may approach that of the natural control of force. These results are the first that demonstrate the feasibility and validity of a non-invasive direct neural interface with the spinal cord, with wearable systems and matching the neural information flow of natural movements.

***Index Terms*— Deconvolution, high-density EMG, human-machine interfaces, motoneurons, motoneuron control, neural interfacing.**

I. Introduction

Interfacing with neural cells in the brain, spinal cord or peripheral nerves usually requires implanted devices [1]–[3], which poses limitations for its widespread applicability. Non-invasive neural interfacing, such as achieved with electroencephalography (EEG), conventionally does not target single neural cell activities and provides limited reliability and poor information transfer rates. Among the target cells for neural interfacing, spinal motoneurons are unique in that their spiking activity can be identified 'remotely' by recording the electrical activity of the innervated muscle tissue [4]. Recordings of the behavior of motor units – the functional quanta of the neuromuscular system, comprising the spinal motoneurons and innervated muscle fibres – have been performed for decades with intramuscular needle or wire electrodes, derived from the original concentric needle electrode [5]. These techniques would potentially enable neural interfacing. However, the identification of the activity of individual motoneurons with intramuscular systems is achieved by highly selective electrodes, so that only a few motoneurons can be investigated concurrently [6], [7]. Because of this limitation, intramuscular electromyogram (EMG) is mainly applied in clinical diagnosis [8] and basic physiological investigations [9], but not as a neural interface.

Recently, it has been shown that multi-channel EMG signals, either recorded invasively [10] or non-invasively [11], can be decoded into the constituent motor unit spike trains, thus providing the means of interfacing with motoneurons using minimally invasive or fully non-invasive (wearable) devices [12]–[14]. These approaches are based on high-density recordings using tens to hundreds of electrodes inserted in the muscle or mounted on the skin, usually referred to as high-density EMG (HDEMG) [12]. Because of the spatial sampling over multiple locations, HDEMG has allowed the identification of tens of motor units concurrently [10], [11], [13]. Thus, it is currently possible to identify and decode the behavior of relatively large samples of the pool of active motoneurons during natural tasks [4], [15]. Moreover, it has been shown that motoneurons can be tracked over long periods of time when the relative location of the recording sites in HDEMG recording systems remains approximately unchanged over time [16].

Beside extending our tools for physiologic and kinesiologic investigations [17], HDEMG has the potential of providing a new means for neural interfacing [18]. For example, we have recently shown that upper limb prostheses can in principle be controlled by the decoded activity of motoneurons [4]. Moreover, since the number of motoneurons controlling human movements is relatively small (i.e. in the order of several thousands) [19] and the input they receive is mostly common to entire pools [20], it has been speculated that it would be feasible to decode the activity of a sufficiently large proportion of motoneurons to extract robust commands for external devices [21]. This hypothesis has been indirectly confirmed in studies associating the statistical characteristics of motoneuron spiking timings to force in natural movements [17]. Nonetheless, the concept of a real-time interface with motoneurons has not been directly validated.

This study was funded by the ERC Synergy Project NaturalBionicS (810346), the EPSRC Centre for Doctoral Training in Neurotechnology and Health, and the Slovenian Research Agency (projects J2-1731, L7-9421 and Programme funding P2-0041).

D. Y. Barsakcioglu, M. Bräcklein, and Dario Farina is with Neuromechanics and Rehabilitation Technology Group, Department of Bioengineering, Imperial College London, London, U.K (correspondence e-mail: d.farina@imperial.ac.uk). A. Holobar is with Faculty of Electrical Engineering and Computer Science, University of Maribor, Maribor, Slovenia.

Here, we focus on non-invasive HDEMG with the aim of proposing a neural interface with ease of deployment. For this purpose, we first present a novel computationally efficient algorithm that allows real-time accurate and reliable decoding of motoneuron activity from HDEMG signals recorded from the skin surface. The technique is based on a blind-source separation approach which separates signal mixtures into the constituent components. We then validate this interfacing approach by comparing its accuracy with both offline decoding as well as with concurrently recorded intramuscular EMG signals as reference. This provides the first direct validation of real-time non-invasive identification of motoneuron activities. We then apply the validated interface in a series of studies involving real-time feedback on the decoded motoneuron activities. Finally, we show that this interface allows an accuracy in control which is close to that achieved when naturally modulating muscle force. Overall, these results – together with the computational efficiency of the proposed algorithm - demonstrate the feasibility, validity and efficacy of a wearable system that interfaces the output circuitries of the spinal cord. Such wearable interfaces with the spinal cord have a wide range of potential future applications, including for rehabilitation systems, prosthetics, sports and ergonomics, as well as fast diagnostic tools for the clinical sector [18].

II. METHODS

A. Online decomposition

We developed a fully automated real-time surface EMG decomposition algorithm. Its high-level block diagram is shown in Fig. 1. It comprises an analogue front-end (AFE), a training module (TM), and a real-time decomposition module (RTDM). The analogue front-end in this study was a commercial system (Quattrocento, OT Bioelettronica, Turin, Italy), while the remaining modules were customized and implemented in Matlab R2017b.

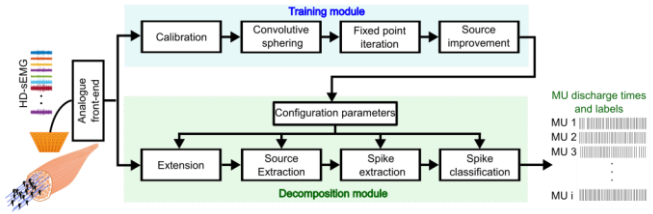

Fig. 1. High-level block diagram of the real-time surface EMG decomposition system. The system comprises an analogue front-end (AFE), a training module (TM), and real-time decomposition module (RTDM). TM performs the computationally demanding tasks of blind source separation and is performed as a one-time procedure (unless a re-training command is issued by the system). Having established real-time parameters through the training module, the RTDM performs real-time extraction of the discharge times of the detected spinal motoneurons. "Extension" block: signals are extended by a factor f_e; "Source extraction" block: extended signals are multiplied by the separation matrix to extract the source signals corresponding to each motoneuron; "Spike extraction" block: the local peaks of the extracted source signals are detected; the detected peaks are classified into signal and noise clusters; the time position of the local peaks assigned to a signal cluster is registered as a valid motoneuron discharge time; "Convolutive sphering" block: it comprises Extension sub-module and whitening of the extended signals; "Fixed point iteration" block: it determines the separation vectors used to extract motoneuron sources; "Source improvement" block: optimisation of the separation vectors. For detailed discussion of each block, please see Section II-A.

The developed system utilizes convolutive blind source separation techniques [11], [22] for identifying motor units and computing a separation matrix to extract motor unit activity from the recoded surface EMG. The separation matrix is computed, by the TM, from EMG recordings in an offline algorithm training phase. This computation involves convolutive sphering of the recorded EMG during which signals are temporarily extended by an extension factor f_e (in order to increase the ratio of number of observations to number of sources) and whitened [11], [22]. It was shown in previous offline studies that the decomposition performance was similar for a range of f_e values tested (i.e., between 8 and 31) and the overall performance did not improve beyond $f_e = 16$ [11]. The factor f_e was therefore defined as $nearest\ integer(1000/N)$, where N was the number of channels. This allowed for optimal performance for $N = 64$ ($f_e = 16$), which was the number of channels used in this study.

Extension and whitening procedures are then followed by a fixed-point iteration algorithm, with a contrast function optimizing the sparsity of the extracted independent sources, to extract separation vectors $\boldsymbol{s_i}$ for each estimated motor unit spike train $\boldsymbol{st_i}$. A second iterative procedure (i.e. source improvement), which estimates the motor unit spike trains with spike detection and *K*-means classification (signal and noise classes), is utilized to further refine the estimations of $\boldsymbol{s_i}$ and $\boldsymbol{st_i}$. This procedure optimizes a separation vector from the estimated discharge timings until reaching a minimum discharge variability, computes a silhouette measure (SIL), and accepts the separation vector $\boldsymbol{s_i}$ as valid if SIL>0.9 [11]. Similar to pulse to noise ratio (PNR) [23], the silhouette measure was proposed as an indicator of reliability [11]. It is computed as the difference between the sum of point-to-centroid distances within cluster and between clusters, divided by the maximum of the two values [11]. In addition to computing a separation matrix $\boldsymbol{S}$ consisting of separation vectors $\boldsymbol{s_i}$, TM also computes spike ($\mathbf{tc_i}$) and noise cluster centroids ($\mathbf{nc_i}$) for each source.

RTDM uses the parameters computed by TM to decompose HDEMG signals in real-time, converting them into a series of motoneuron action potential discharge timings (i.e. spike trains). During the real-time operation, the recorded HDEMG signals are extended. In contrast to TM, the extended sources are not spatially whitened during real-time operation in order to reduce the computational load associated with the computation of the whitening matrix arising from the singular value decomposition needed for whitening. Instead, the real-time separation matrix is designed to operate on extended unwhitened observations. This is achieved during the training phase where a whitening matrix $\mathbf{W}$ is computed, and the extracted separation vectors are transformed using $\mathbf{W}$.

Following extension, the source trains ($\boldsymbol{st_i}$) are extracted by multiplying the extended observations with the real-time separation matrix. The local peaks of squared source trains ($\boldsymbol{st_i^2}$) are detected. A local peak is defined as a data sample that is larger than its neighboring samples. The Euclidean distances of each detected local peak from $\mathbf{tc_i}$ and $\mathbf{nc_i}$ are computed. Each peak is then classified by the spike classification unit,

based on the computed distances, either as corresponding to discharge of a motor unit or as noise. Finally, the time occurrence (i.e. timestamp) of each detected motor unit spike is output along with information about which motor unit it belongs to (i.e. spike label).

The computational requirements of the proposed system were quantified both as number of computations per sample (in terms of system parameters) and measurements in time under various conditions in order to ensure real-time performance. In the proposed system, the training module (TM) performs the computationally demanding tasks of blind source separation which is performed once. Having established many of the system parameters through the training module, the RTDM requires minimal computations to extract motor unit activities in real-time. The computational complexity of the RTDM, as presented in Table I, mainly depends on the number of channels (N) and the number of identified motor units (M).

The source extraction sub-module is the most computationally demanding part of RTDM as it requires vector multiplications to extract the spikes of each detected motor unit. Assuming typical high-density electrode channel counts (i.e. 64, 128, and 192 channels), and 20 extracted motor units, the real-time decomposition module requires for each acquired sample, 27 additions, 347 multiplications, 16 shifts, and 32 comparisons for the worst case scenario. The worst case scenario assumes that one out of every three samples of each ***st$_i$***, received by *Spike* extraction processing block, corresponds to a local peak. Since the extracted local peaks consist of actual spike discharges of motor units, which is a function of individual firing rate of each motoneuron, and the noise which is of random nature, we only report the worst case in Table I.

TABLE I
COMPUTATIONAL REQUIREMENTS OF THE REAL-TIME DECOMPOSITION MODULE QUANTIFIED BY THE NUMBER OF OPERATIONS (IN SYSTEM PARAMETERS) REQUIRED PER SAMPLE RECORDED.

Processing block	Add	Multiply	Shift	Compare
Extension	-	-	f_e	-
Source Extraction	f_e	M.f_e	-	-
Spike extraction	-	f_e	-	2.f_e–2/N
Spike classification	2.N.f_e/3	2.f_e/3	-	-

N is the number of HDEMG channels and M is the number of detected motor units. Let $\lfloor x \rceil$ denote the nearest integer function. $f_e = \lfloor 1000/N \rceil$ is the extension factor.

Using synthetically generated HDEMG [24], the computational time of the RTDM module was measured for varying number of recording channels (from 64 to 192 channels) across various analogue front-end (AFE) buffer sizes (from 1 to 256 samples/channel). For the measurements, a system with Intel Core i7 2.6GHz, 16GB RAM was used. From these analyses, the maximum average computational time (i.e., maximum latency) was 3.4 ± 0.43 (0.06 - 4.3) ms for a 192-channel system that utilizes an AFE buffer size of 256 samples/channel. For the case of the AFE used in this study, the minimum available buffer size of 128 samples and a sampling rate of 2048 Hz were chosen (i.e. fixed acquisition latency of 62.5ms). Together with the corresponding measured real-time decomposition latency for 64-channels (i.e. 0.65 ms), the overall latency for acquisition and processing the signals was less than 64 ms (excluding ethernet communication). This allows up to 140 ms for extra computation and visualization time while still ensuring overall latency is below 200 ms [25], [26].

B. *Experiments*

For all the experiments, HDEMG signals were recorded using 64-electrode adhesive grids (5 columns and 13 rows; gold coated; OT Bioelettronica, Torino, Italy) mounted over the belly of the target muscle. For tests on the tibialis anterior and extensor digitorum muscles, a high-density electrode array with an 8-mm inter-electrode distance was used; for tests on the first dorsal interosseus and abductor digiti minimi muscles a smaller sized high-density electrode array with an inter-electrode distance of 4-mm was applied. A conductive paste was used to improve the electrode-skin contact. Before the placement of the electrode array, the skin above the target muscle was shaved and cleansed with abrasive paste and ethanol. The signals were recorded in monopolar derivation with a Quattrocento Amplifier (OT Bioelettronica, Torino, Italy), analogue band-pass filtered (10 – 500 Hz) for signal conditioning and anti-aliasing, sampled at 2048 Hz and A/D converted to 16 bits. The force was measured through CCT TF-022 force transducer and recorded, amplified (OT Bioelettronica, Torino, Italy), and band-pass filtered (0 – 30 Hz).

A Matlab-based implementation of the real-time decomposition system, as described above, together with a custom designed graphical user interface (GUI) was used during the experiments. The GUI provided real-time feedback on either force, spiking activity of individual motor units, or cumulative spike trains (CST) of sets of motor units (Fig. 2). The spiking activity feedback presented a real-time raster plot (i.e. spike train) of all detected motor units (Fig. 2A). The

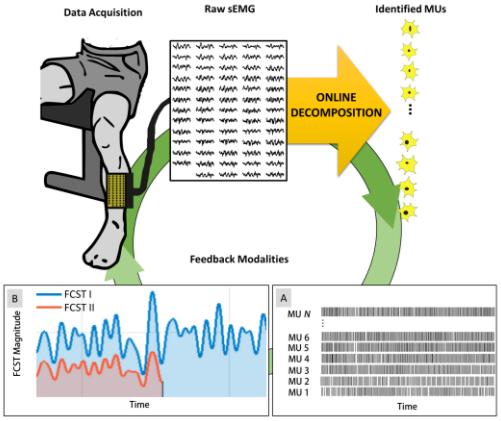

Fig. 2. Closed-loop biofeedback on motoneuron activity. Schematic overview of the feedback and pre-processing chain used in all experiments. TOP: Data acquisition from the target muscle via HDEMG and real-time decoding of the underlying motoneuron activity. BOTTOM: Participants received visual feedback either on single motor unit spiking (A) or on two filtered cumulative spike trains (FCSTs) (orange and blue line; see main text for details) (B), depending on the experimental tests. The user can adjust the range of time axis display, as well as the update rate of the GUI. The GUI update rate is dependent on the acquisition parameters chosen by the user. Please refer to section II-A for discussion of the latency.

CSTs are constructed by summing the spike trains of two or more motor units. The GUI allows experimenter to produce a single CST based on all decoded motor units or define multiple CSTs based on various subsets of decoded motor units, as well as allowing several filtering options (i.e. filter order, cut-off frequencies, filter type) to generate a filtered cumulative spike train (FCST), as shown in Fig. 2B.

For all the experiments, participants started with performing a maximum voluntary contraction (MVC) force in dorsiflexion, abduction or extension, depending on the recorded muscle. The maximal contraction was followed by ramp contractions that comprised a 4 s ramp trajectory at 2.5 % MVC/s, and a 10% MVC sustained contraction over 41 s. During this initial phase, participants were always presented with the overall force feedback. HDEMG signals recorded during the ramp contraction were used as the calibration data for the decomposition system to identify motor units and real-time decomposition system parameters. The participants were then asked to slowly recruit one motor unit after another by increasing the contraction level from 0 % to 10 % MVC while single motor unit spiking activity of the entire pool was visually presented. This test, which lasted 10-15 s, verified that the participants could effectively use the visual feedback on motoneurons. All participants were able to directly use the interface in an intuitive way.

In this study, we selected relatively low force contraction levels for multiple reasons. For the presented validation with intramuscular EMG recordings, the force needs to be low for limitations of the invasive methods that require the activation of a small number of units. For the tests on force control, low contraction levels are associated to large physiological force variability and therefore they are the most challenging from a control perspective (this is reflected by the relatively high force variability reported in our results in Section III-D). Finally, higher force levels are associated to muscle fatigue that we wanted to avoid in all tests.

All experimental procedures were approved by Joint Research Compliance Office under the Imperial College Research Ethics Committee process (reference 18IC4685). All participants gave informed consent according to procedures approved by the ethics committee at Imperial College London. The participants were naive volunteers and did not undergo any training prior to or during the experiments.

C. Study I: Accuracy of online vs offline decomposition

HDEMG of the tibialis anterior muscle of eight healthy participants (3 females, 5 males; age: 27.8 ± 5.5 yrs) were recorded. Additional experiments were performed on the tibialis anterior, first dorsal interosseus, abductor digiti minimi, and extensor digitorum muscles of one healthy participant (male, 28). For the tibialis anterior muscle, the foot was fixed into position using an ankle dynamometer (NEG1, OT Bioelettronica), with the ankle flexed at 0º, to allow isometric dorsiflexion of the ankle. For the measurements on the upper limb, i.e. abduction of the index finger (first dorsal interosseus), abduction of the little finger (abductor digiti minimi), and extension of the medial four digits of the hand (extensor digitorum), a custom designed experimental setup was used to fix the forearm, the wrist and the hand. It consisted of an adjustable-height platform to ensure the forearm was bent at the elbow at 90º and the hand was pronated at 90º. The force sensor platform was adjusted accordingly and fixed ensuring the digits of the hand relevant to the measurement stayed in contact with the force platform at rest.

During the experiments, visual feedback on the discharge behaviour of each identified motor unit (i.e. spiking activity feedback) was provided. Participants were asked to recruit all identified motor units and to sustain a constant firing rate for 45 s at a contraction force of approximately 10 % MVC. The MVC % force level, in this case, was also displayed through the GUI.

For the offline analysis, the HDEMG signals were processed with an offline decomposition algorithm [11] to assess the overall quality of the online decomposition. The offline decomposition was performed with a threshold of SIL > 0.9, while the fixed-point algorithm was iterated over 50 times [11]. The results of the offline decomposition were manually edited for maximizing the accuracy. To quantify the performance of the real-time decomposition to the offline benchmark, the rate-of-agreement (RoA) was used as a metric:

$$RoA\ \% = \frac{c_j}{c_j + RT_j + OL_j} \times 100\ \% \quad (1)$$

where c_j is the number of discharges of the j^{th}motor unit identified by both real-time and offline decomposition algorithms, RT_j is the number of discharges identified by the real-time system only, and OL_j is the number of discharges identified by offline decomposition only.

D. Study II: Accuracy of online decomposition: two-source validation

For further validation of the online decomposition, with the two source method, concurrent intramuscular EMG (iEMG, measured with a pair of wire electrodes inserted into the muscle with a 25G needle) and surface HDEMG signals (measured with a 5×12 electrode array, 5 mm interelectrode distance) recorded from the tibialis anterior muscle of 12 men (age: 27 ± 3.5 yrs) during previous studies were used [14]. The recordings used consisted of 20 s isometric contractions of 5%, 10% and 15% of the MVC. The surface HDEMG signals were bandpass filtered (10-500 Hz) and sampled at 2048 Hz. The intramuscular signals were bandpass filtered (0.5-5 kHz) and sampled at 10 kHz. The iEMG signals were decomposed into sources using EMGLab [27], which is an established offline decomposition algorithm for intramuscular EMG signals. For these tests, the online surface EMG decomposition algorithm was simulated in an offline way to decompose the HDEMG. The HDEMG signals were partitioned into two equal datasets. One dataset was used to train the system parameters, while the remaining dataset was fed into the simulated RTDM. This was then repeated by interchanging the training and testing datasets. The recordings were only considered for analysis if the offline decomposition provided at least one source which had a RoA with the corresponding intramuscular recording above or equal to 75%.

The recordings that did not meet this criterion were discarded. This criterion was based on the need to match the motor units detected from the intramuscular and surface recordings since there is no way of deciding on the association without a criterion based on the correspondence of discharges. The RoA provided for the matched units (see Section III-B) were well above 80-90% and thus very distant from the threshold used for matching, indicating a bias has not been introduced as a result of this matching criterion.

E. Study III: Common input to motoneurons

Experiments were performed on 11 healthy participants (1 female, 10 male; age: 25.1 ± 2.2 yrs). HDEMG from the tibialis anterior muscle was recorded while the foot was locked into position to measure isometric dorsiflexion of the ankle only.

The HDEMG signals acquired during a 40 s window of an isometric contraction at 10% MVC were decomposed into active motor unit spiking and labelled as force control condition, i.e. a control condition in which visual feedback was provided on the generated force. From the set of detected motor units, 12 were selected (in the order of recruitment and ensuring all were active at 10% MVC), and were randomly divided into three sets of four motor units each, labelled as Ctrl-Set, A-Set, and B-Set, respectively. The choice of 12 motor units was based on the minimum number of motor units that we expected to identify during contractions of the TA muscle (from previous empirical evidence obtained with the proposed system) and desire to maintain the same number of motor units across test conditions (i.e. Ctrl-Set, A-Set, and B-Set) and participants. Two FCSTs were then computed as the low-pass filtered (10 Hz, second-order Butterworth filter) versions of the sum of the individual motor unit spike trains in the Ctrl-Set and A-Set (Condition I) and in the Ctrl-Set and B-Set (Condition II). The participants then received visual feedback on the FCST for each condition twice (four trials), with 5 min of rest in between.

The strength of common input received by the motoneurons in the Ctrl-Set and A-Set, as well as in the Ctrl-Set and B-Set was estimated by using the maximum-squared coherence analysis on the de-meaned unfiltered CSTs of the corresponding motor units [28]–[31]. Therefore, the power spectral densities of both CSTs $P_{Ctrl}(f)$ and $P_{A/B}(f)$, as well as the cross power spectral density $P_{CtrlA/B}(f)$ (Hanning window of 1 s, 50 % overlap) determined the estimated coherence value $C_{CtrlA/B}(f)$, as follows:

$$C_{CtrlA/B}(f) = \frac{\left|P_{CtrlA/B}(f)\right|^2}{P_{Ctrl}(f)P_{A/B}(f)} \quad (2)$$

The confidence threshold for the estimated coherence values was:

$$CL = 1 - (1-\alpha)^{\frac{1}{N-1}} \quad (3)$$

with the number of segments N used in the estimation and α = 0.05 as level of confidence [29]. Motor units in the Ctrl-Set were always present in both conditions. The coherence between both pairs of sets was computed for the four trials. The estimated coherence values were averaged in four frequency bands: δ = 1-4 Hz, θ = 4-8 Hz, α = 8-13 Hz, β = 13-30 Hz [32]. The root mean square error (RMSE) between the target FCST and the recorded FCST was calculated and maximum-normed to the presented FCST to evaluate to which degree the participants were able to follow the trajectory.

F. Study IV: Accuracy in voluntary control of motoneuron output

Experiments were performed on eight healthy participants (4 females, 4 males; age: 27.6 ± 5.2 yrs) who also took part in the validation study (Study I; see above). Recordings were performed with HDEMG systems from the tibialis anterior muscle. The foot was locked into position to measure isometric dorsiflexion of the ankle only. During the initial part of the experiment, following initial system calibration, the participants were shown the discharge times of each identified motor unit, decoded in real-time from the tibialis anterior muscle. They were then asked to perform ankle dorsiflexions in order to progressively recruit motor units and then progressively derecruit the activated units for a few minutes to familiarize with the interface (Fig. 2).

TABLE II
DECOMPOSITION ACCURACY OF THE REAL-TIME (I.E. ONLINE) SYSTEM MEASURED WITH 64-CHANNEL HDSEMG RECORDINGS ACROSS TIBIALIS ANTERIOR (TA), FIRST DORSAL INTEROSSEUS (FDI), ABDUCTOR DIGITI MINIMI (ADM), AND EXTENSOR DIGITORUM (ED).

Muscle	No. of MUs	Rate of Agreement %	Average Discharge Rate (pps†)	Average Discharge variability %
TA	12	100 / 0.2 (99.4–100)	11.5 / 2.5 (10.2 – 14.0)	9.5 / 1.3 (8.1 – 13.3)
FDI	5	99.4 / 0.8 (98.3–100)	9.4 / 2.1 (7.9 – 11.2)	11.9 / 2.3 (10.3 – 15.9)
ADM	6	94.2 / 4.4 (93.2–99.1)	16.2 / 10.5 (9.1 – 22.4)	18.0 / 7.9 (13.1 – 5.4)
ED	7	92.6 / 5.5 (87.4–94.8)	17.4 / 4.9 (12.8 – 30.8)	25.2 / 9.0 (14.4 – 28.1)

Rate of Agreement, discharge rate, and discharge variability are given as median / interquartile range (minimum RoA – maximum RoA), across all identified motor units. † pps: pulses per second. Average Discharge variability is computed as coefficient of variation of motoneuron discharge rates.

The participants were then provided a target trajectory to follow with three types of visual feedback: FCST of all detected motor units, amplitude of the EMG, and force. The target trajectory consisted of a 4 s ramp (increasing), followed by a constant level for 32 s at 10 % MVC, and ending with a 4 s ramp (decreasing). All tasks were randomized and repeated twice for each visual feedback type. All visual feedback signals were filtered with a 4th order Butterworth lowpass filter with a cut-off frequency of 5 Hz.

The targets for the neural feedback condition were computed as the average FCSTs corresponding to the force levels in the force feedback condition.

III. RESULTS

We present the results of the four main studies of online control of motoneurons in healthy individuals, as described above. The first study validated the online decoding in several

muscles by comparing the decoded spike trains during real-time control with the signal decomposition manually performed offline with state-of-the-art methods. Since offline, manually verified, decomposition methods have been extensively validated previously [11], [13], this comparison provided an initial proof of the accuracy of the online decoding. Because this validation is still indirect, we further validated the online decoding with the two-source approach [33], which is based on comparing the decomposition of concurrently recorded intramuscular and surface EMG signals of various contraction intensities (second study). The third study investigated spectral coherence between the activities of groups of motoneurons when providing feedback on only a subset of motoneurons and established the stability of the control. The fourth study showed the accuracy in controlling motoneuron recruitment/derecruitment and compared the accuracy in 1D control of motoneuron output with that of conventional EMG and force control.

A. Study I: Accuracy of online vs offline decomposition

The accuracy was first tested in eight participants on the tibialis anterior muscle. The tests were performed by providing spiking activity of identified motoneurons (i.e. a real-time raster plot) as visual feedback to the participants and requesting them to progressively recruit motoneurons, to maintain their activity for approximately 10 s, and then to progressively derecruit motoneurons. The result of the online decomposition was also stored and compared with the subsequent offline, partly manual decomposition. The accuracy was quantified RoA between online and offline decomposition (see Methods). For the tibialis anterior muscle, the median rate of agreement across the eight participants between offline and online decomposition was 95.5% (interquartile range: 7.9 %, min. 37.3 %, max. 100%).

Further tests of accuracy were then conducted in several muscles for one participant. These additional tests were performed on the tibialis anterior, first dorsal interosseus, abductor digiti minimi, and extensor digitorum muscles, as representative muscles of the lower and upper limb. Across these muscles, the online decomposition identified 5 to 12 motor units. Table II reports the rate of agreement between online and offline (partly manual) decomposition as well as the discharge rate and discharge variability of the identified motor units for all muscles. The values of agreement are >90% for all muscles and are similar across muscles. The values for discharge rate and discharge variability are in agreement with known physiological values [34].

These results indirectly indicate high accuracy of the online identification of motoneuron spiking and generality of the approach to muscles with different architectures and control properties. Nonetheless, this validation is indirect as it relies on the assumption that offline decomposition is accurate. While the latter has been verified in previous studies [11], [14], [22], here we further tested the validity of the online decomposition in a direct way.

TABLE III
DECOMPOSITION ACCURACY OF THE REAL-TIME (I.E. ONLINE) SYSTEM VALIDATED WITH THE TWO-SOURCE METHOD USING CONCURRENT INTRAMUSCULAR AND SURFACE HDEMG RECORDINGS FROM THE TIBIALIS ANTERIOR MUSCLE.

Participant No	%MVC	No. of motor units matched		Rate of agreement %	
		Offline	Online	Offline	Online
1	10	1±0	1±0	99.1±0	96.3±1.3
	10	1±0	1±0	88.7±0	83.2±7.6
	5	1±0	0.5±0.7	99.0±0	95.1±0
	5	1±0	1±0	99.1±0	94.5±1.9
2	15	1±0	1±0	86.5±0	79.9±1.9
3	15	1±0	1±0	92.7±0	87.5±6
	5	1±0	0.5±0.7	99.3±0	90.5±0
	5	1±0	1±0	96.8±0	90.6±1.1
4	10	1±0	2±0	98.0±0	96.8±1.2
	10	1±0	1.5±0.7	97.7±0	95.9±3.6
	15	2±0	2.5±0.7	97.6±0.7	91.0±8.4

The rate of agreement between decomposed HD-sEMG recordings with the proposed real-time system and decomposed intramuscular EMG recordings is presented. For comparison, the rate of agreement between decomposed HD-sEMG recordings with an offline algorithm and decomposed intramuscular EMG recordings is also presented.

B. Study II: Accuracy of online decomposition: two-source validation

Among all methods proposed for assessing the accuracy of decomposing non-invasive EMG signals, the most direct one is the comparison of the decomposition results with those obtained decomposing concurrently recorded intramuscular EMG signals [33]. According to this approach, the rate of agreement is computed between spike trains decomposed from different signals (intramuscular and surface) and with different decomposition methods. The rationale for the approach is that the likelihood that the two decompositions provide exactly the same errors is extremely small and therefore the rate of agreement is a conservative estimate (i.e., it underestimates) of the decomposition accuracy.

To test the validity of online decomposition with the two-source method, we used intramuscular EMG and surface HDEMG signals recorded from the tibialis anterior muscle in our previous studies [14]. These previously recorded surface HDEMG signals were decomposed by simulating the online processing. For this purpose, the surface HDEMG signals were partitioned into two equal datasets (i.e. train/test split method), where one dataset was used as the training dataset while the other was the test dataset. This was then repeated by switching the test and training datasets.

The RoA between the intramuscular and surface decompositions was on average 91.5 ± 6.6% (1.2 ± 0.7 matching motor units per recording; this number of matched motor units is in agreement with previous studies, i.e. 1 ± 1 units were matched in previous studies, using the two-source method for validating offline decomposition [14]), with individual subject results presented in Table III**.** Moreover, the offline algorithm was also applied to the full recordings (i.e. trained on the whole dataset) for comparison. The RoA between offline surface HDEMG decomposition and the decomposed intramuscular data was 96.0 ± 4.3 (1.1 ± 0.3 matching motor units per recording).

The validation with the two-source method, together with the comparison with the offline decomposition, provides a solid proof of the accuracy of the proposed approach in a variety of muscles.

C. Study III: Common input to motoneurons

Motoneuron pools receive a large proportion of common synaptic input [35], [36]. This control strategy is needed for accurate control of muscle force [37], [38]. The presence of common input signal to relatively large groups of motoneurons allows estimating the input by decoding only a fraction of the active motoneurons, so that a relatively small proportion of decoded neurons is representative of a large pool. The presence of common input to motoneurons has been extensively proven experimentally [39]. Nonetheless, it has not been demonstrated when controlling motoneurons via feedback, as in neural interfacing. Therefore, here we analysed spectral coherence between groups of motoneurons when providing feedback on only a subset of decoded motoneurons.

Eleven healthy participants completed the experiment. For each participant, a set of 12 motor units online identified from the tibialis anterior muscle was randomly divided into three sets of four motor units each - labelled as Ctrl-Set, A-Set, and B-Set – and computed the corresponding CST for each set of motor units. The CSTs were filtered in the effective bandwidth of control (see Methods) to obtain FCSTs. Participants received visual feedback on the FCSTs derived from the motoneurons in the A- and Ctrl-Set (Condition I) and in the B- and Ctrl-Set (Condition II). Participants were instructed to follow a target level to be matched with the FCST in each condition. A control condition in which visual feedback was provided on the generated force, instead of on the FCSTs, was also included. The maximum-squared coherence between unfiltered CSTs was used to assess the strength of common input between the three sets of motoneurons in the three feedback conditions (Condition I, II, and force control).

In total, 150 motor units were identified online (on average, 13.63 ± 2.11 per participant; minimum of 12 motor units per participant). The RMSE between the target and the FCST was used as a measure of control accuracy. The global error across the entire sample was 11.32 ± 1.62 % of the maximum amplitude of the corresponding FCST. Furthermore, a paired-samples t-test was conducted to compare the RMSE depending on the subset of motoneurons provided as feedback (Condition I: 11.45 ± 1.70 %; Condition II: 11.18 ± 1.57 %) and no significant difference was detected ($t(42) = 0.55$, $p > 0.5$), which suggested that the accuracy in control of the FCST did not depend on the motoneuron set used for the visual feedback. Notably, the subjects did not need any training when suddenly switching from one set of motoneurons for feedback to the other. They naturally switched and performed the required task with similar accuracy in all conditions.

Fig. 3 shows the spectral coherence functions between the sets of motoneurons when varying the feedback condition. A Kruskal-Wallis test revealed no significant effect of the feedback condition on the estimated level of received common input (δ band: $H(5) = 5.66$, $p > 0.3$; θ band: $H(5) = 1.58$, $p > 0.9$; α band: $H(5) = 2.7$, $p > 0.7$; β band: $H(5) = 1.04$, $p > 0.9$). Therefore, the set of motor units excluded from the feedback in each condition acted coherently with those used for feedback, indicating that the feedback on one sub-set of motoneurons acted on the entire pool of motoneurons.

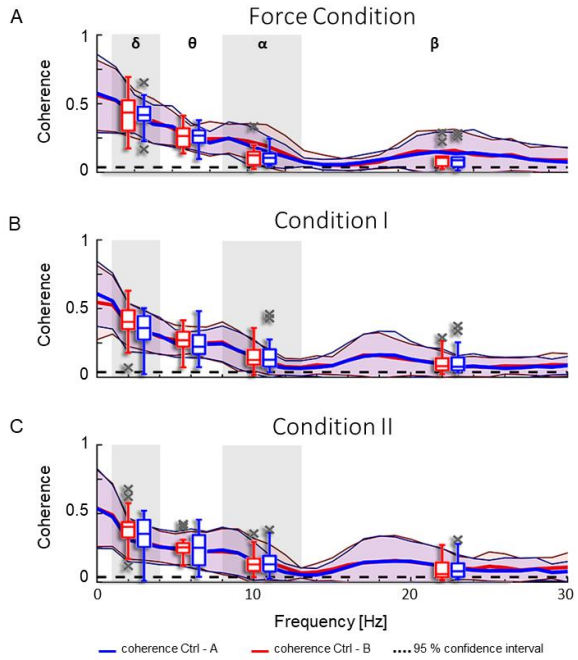

Fig. 3. Spectral coherence analysis for various visual feedback modalities. The coherence functions are computed with their mean and standard deviation (shaded areas around line plot) between cumulative spike trains extracted from the Ctrl-set and A-subset (blue line), and from the Ctrl-set and B-subset (red line) for the conditions of force feedback (A), and filtered cumulative spike trains feedback (B and C). The averaged coherence values in the δ, θ, α, and β frequency bands are shown by their medians and quartiles. The dashed black line indicates the 95 % confidence interval of the coherence estimate in each condition.

These results show that online feedback on a relatively small set of motoneurons is representative of the control of the entire motoneuron pool (as the motoneurons not provided as feedback behaved coherently with those provided as feedback). The results may also suggest that a neural interface based on feedback on motoneurons might remain stable even if some of the motoneurons identified over time would change, as it was experienced by the subjects in this experiment. Nevertheless, further experimentation is required to investigate the latter point.

D. Study IV: 1-D control

We then investigated the ability to proportionally control a 1-D signal by motoneuron activity and compared the variability in control with respect to EMG-based and natural force control. A total of eight participants were recruited for this experiment and surface HDEMG was recorded from the tibialis anterior muscle during ankle dorsiflexion.

The participants were provided with three modes of visual feedback. The neural feedback was the FCST of the motor units decomposed in real-time. With this feedback, the participants were asked to follow, as closely as possible, a trajectory at 10% of the maximal voluntary contraction. The force and EMG feedbacks were based on force and estimated EMG amplitude, respectively, at the same relative levels used for the neural feedback. The control task was repeated twice by each participant.

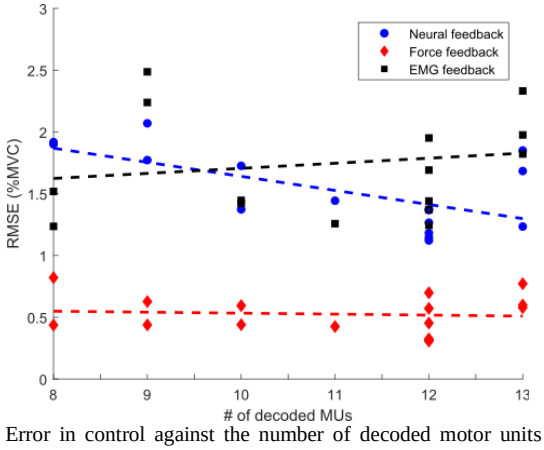

Fig. 4. Error in control against the number of decoded motor units under neural (blue circle markers), emg control (black square markers), and force control (red diamond markers). The root mean squared error in control was analysed as a function of the number of decoded (i.e. identified by the decomposition) motor units across all trials and participants. Linear regression curves for neural control (blue dashed line), EMG control (black dashed line) and force control (red dashed lines) are also presented. The error in control with neural feedback decreased with the number of decoded motor units as expected theoretically. As also expected, EMG and force control does not depend on the number of decoded units.

On average, 11.8 ± 2.3 motor units were decomposed per participant (minimum 8 motor units and maximum 15 motor units). Force feedback had lower overall CoV (mean variability of 4.4 ± 1.5 %) and RMSE (mean error of 0.5 ± 0.2 % MVC) across participants compared to the variability resulting from both the EMG and the neural feedback, but neural feedback led to higher precision (mean variability of 13.8 ± 2.1% and RMSE of 1.5 ± 0.3 % MVC) than EMG-based feedback (mean variability of 17.0 ± 4.7 % and RMSE of 1.7 ± 0.5 % MVC). Moreover, the error in control with neural feedback decreased with the number of decoded motor units, as expected theoretically [21], so that there was a negative correlation between RMSE and number of decoded units (R=-0.64 and P=0.008; Fig. 4). EMG (R = 0.15 and P= 0.56) and force (R = -0.09 and P=0.79) control did not depend on the number of decoded units, as expected.

IV. DISCUSSION

We have developed a fully automated non-invasive neural interface with the output circuitries of the spinal cord that provides real-time feedback on motoneuron spiking activities. The interface has been extensively validated and demonstrated in experiments on human participants that showed accurate, intuitive, and robust control of motoneuron output in untrained individuals.

The proposed interface is based on developments in HDEMG analysis of the last two decades [11], [13], [14], [40]. The key contributions of the present work are 1) the novel online decomposition algorithm; 2) the first direct validation of online decomposition by comparison with intramuscular decomposition; 3) the demonstration that motoneurons behave coherently during a feedback task; and 4) the demonstration, during a 1D control task, that the accuracy in control of the proposed interface is superior to that of conventional myocontrol.

Accuracy of the developed interface has been first shown by comparison of the online motoneuron decoding with the offline approach. The offline approach to surface EMG decomposition has been previously extensively validated [11], [12], [14], and therefore could be used as reference for accuracy assessment. The rate of agreement between offline and online decomposition was in all cases >90%, indicating high performance of the online implementation. In a second step, we provided a more direct validation of online decomposition by comparison with concurrently recorded and independently decomposed intramuscular EMG signals. This further test revealed similar RoA as for the comparison with offline decomposition (~90%) and provided ultimate evidence of the high accuracy of the online interface.

The validation tests were followed by two studies that provided evidence that the interface can be used intuitively without subject training. We first tested the ability of participants to control different sets of motor units interchangeably. This test served to prove both the robustness of the interface and its stability. Indeed, it proved that participants could control any sets of motoneurons without (re)training. The switch in control from one set to the other was immediate and natural, and the participants did not experience any difficulties when changing the set of motoneurons. The error in control was indeed similar across conditions. Moreover, motoneurons whose activity was not provided as feedback showed a behavior highly coherent with those used for feedback. Indeed, the coherence of a set of motoneurons with the control set of motoneurons was the same irrespective of whether the set was used as feedback or not. This is consistent with the well-known notion that pools of motoneurons receive a strong proportion of common input [39]. This notion has been tested here for the first time with biofeedback on groups of motoneurons. The behavior of the motoneurons provided as feedback was representative of the behavior of the entire motoneuron pool, including neurons not provided as feedback. For interfacing, this result indicates that the interface would work in a stable way over multiple uses, even if the identified motoneurons would change at each use.

Finally, we tested the proposed system in a 1D control experiment. We compared the proportional command signal extracted from the activity of motoneurons with both force and EMG amplitude. For these comparisons, we chose a relatively low force level, which is known to correspond to relatively large force variability [34] and which therefore challenged the interface. The command extracted from motoneuron activity led to greater variability than force control but lower than EMG amplitude control. Moreover, the accuracy in control improved when the number of decoded motor units increased (Fig. 4), as expected from the physiological principles of force generation [37]. It has been shown that force generation is linearly dependent on the neural drive (i.e. cumulative spike trains) to the muscles [20], [37]. The pool of motor neurons act as a linear selective filter that eliminates non-common components of the synaptic input. The greater the number of detected motor units by the proposed interface, the more accurate is the estimate of the neural drive (i.e. hence intended force output). In the 1D control experiment, we demonstrated that the proposed interface has the potential of surpassing the accuracy in force estimation based on EMG amplitude and

matching the stability of force control when a sufficient number of motoneurons is decoded [35], [37]. This provides a large margin of improvement based on advances in decomposition accuracy and number of extracted spike trains.

While it is in principle possible to extract features associated with the cumulative spike train to build control signals, currently there are no robust methods that can extract accurately the number of discharges per unit time of a subset of active units without first decomposing the signal fully. Moreover, in applications where it is needed to distinguish the activity of muscles closely spaced, single motor units must be resolved and assigned to specific degrees of freedom, which is not possible from the total number of discharges per unit time. Finally, some physiological investigations would still require feedback on single motor units (as opposed to the full neural drive), such as when assessing the possibility for the central nervous system to disentangle the control of motor units in the same pool.

V. Conclusion

In conclusion, we provided a neural interface that can be mounted non-invasively on the skin surface and that provides highly accurate identification of spiking times of spinal motoneurons in real-time. We provided a first direct validation of real-time non-invasive identification of motoneuron activities by comparing its accuracy with both offline decoding and concurrent intramuscular EMG signals. We further tested the proposed interface in a series of studies involving real-time feedback on the decoded motoneuron activities. With this interface, naïve participants could control in real time motoneuron activity in tasks involving proportional commands without training. Moreover, the participants could produce voluntary control commands switching from one set of neurons to another intuitively and without the need for any learning period. This interface has potential applications in technologies that requires accurate transfer of information with the human nervous system, such as rehabilitation devices.

References

[1] F. R. Willett *et al.*, “A comparison of intention estimation methods for decoder calibration in intracortical brain-computer interfaces,” *IEEE Trans. Biomed. Eng.*, vol. 65, no. 9, pp. 2066–2078, 2018.

[2] B. Jarosiewicz *et al.*, “Virtual typing by people with tetraplegia using a stabilized, self-calibrating intracortical brain-computer interface,” *IEEE BRAIN Gd. Challenges Conf. Washington, DC*, vol. 7, no. 313, pp. 1–11, 2014.

[3] G. Santhanam, S. I. Ryu, B. M. Yu, A. Afshar, and K. V Shenoy, “A high-performance brain–computer interface,” *Nature*, vol. 442, no. 7099, pp. 195–198, Jul. 2006.

[4] D. Farina *et al.*, “Man/machine interface based on the discharge timings of spinal motor neurons after targeted muscle reinnervation,” *Nat. Biomed. Eng.*, vol. 1, no. 2, p. 0025, Feb. 2017.

[5] E. D. Adrian and D. W. Bronk, “The discharge of impulses in motor nerve fibres,” *J. Physiol.*, vol. 67, no. 2, pp. 9–151, 1929.

[6] C. J. De Luca and W. J. Forrest, “An electrode for recording single motor unit activity during strong muscle contractions,” *IEEE Trans Biomed Eng*, vol. 19, no. 5, pp. 367–372, 1972.

[7] J. V. Basmajian and G. Stecko, “A new bipolar electrode for electromyography,” *J. Appl. Physiol.*, vol. 17, no. 5, pp. 849–849, 2017.

[8] E. Stålberg, “New EMG methods to study the motor unit.,” *Electroencephalogr. Clin. Neurophysiol. Suppl.*, vol. 39, pp. 38–49, 1987.

[9] C. J. De Luca, R. S. LeFever, M. P. McCue, and A. P. Xenakis, “Behaviour of human motor units in different muscles during linearly varying contractions,” *J. Physiol.*, vol. 329, no. 1, pp. 113–128, Aug. 1982.

[10] S. Muceli *et al.*, “Accurate and representative decoding of the neural drive to muscles in humans with multi-channel intramuscular thin-film electrodes,” *J. Physiol.*, vol. 593, no. 17, pp. 3789–3804, 2015.

[11] F. Negro, S. Muceli, A. M. Castronovo, A. Holobar, and D. Farina, “Multi-channel intramuscular and surface EMG decomposition by convolutive blind source separation,” *J. Neural Eng.*, vol. 13, no. 2, p. 026027, 2016.

[12] A. Holobar, D. Farina, M. Gazzoni, R. Merletti, and D. Zazula, “Estimating motor unit discharge patterns from high-density surface electromyogram,” *Clin. Neurophysiol.*, vol. 120, no. 3, pp. 551–562, 2009.

[13] A. Holobar and D. Farina, “Blind source identification from the multichannel surface electromyogram,” *Physiol. Meas.*, vol. 35, no. 7, pp. R143–R165, 2014.

[14] A. Holobar, M. A. Minetto, A. Botter, F. Negro, and D. Farina, “Experimental analysis of accuracy in the identification of motor unit spike trains from high-density surface EMG,” *IEEE Trans. Neural Syst. Rehabil. Eng.*, vol. 18, no. 3, pp. 221–229, 2010.

[15] V. Glaser and A. Holobar, “Motor unit identification from high-density surface electromyograms in repeated dynamic muscle contractions,” *IEEE Trans. Neural Syst. Rehabil. Eng.*, vol. 27, no. 1, pp. 66–75, 2019.

[16] E. Martinez-Valdes, F. Negro, C. M. Laine, D. Falla, F. Mayer, and D. Farina, “Tracking motor units longitudinally across experimental sessions with high-density surface electromyography,” *J. Physiol.*, vol. 595, no. 5, pp. 1479–1496, 2017.

[17] D. Farina, F. Negro, S. Muceli, and R. M. Enoka, “Principles of Motor Unit Physiology Evolve With Advances in Technology,” *Physiology*, vol. 31, no. 2, pp. 83–94, 2016.

[18] D. Farina and A. Holobar, “Human-machine interfacing by decoding the surface electromyogram,” *IEEE Signal Process. Mag.*, vol. 32, no. 1, pp. 115–120, 2015.

[19] B. Gesslbauer, L. A. Hruby, A. D. Roche, D. Farina, R. Blumer, and O. C. Aszmann, “Axonal components of nerves innervating the human arm,” *Ann. Neurol.*, vol. 82, no. 3, pp. 396–408, 2017.

[20] F. Negro, U. Ş. Yavuz, and D. Farina, “The human

motor neuron pools receive a dominant slow-varying common synaptic input," *J. Physiol.*, vol. 594, no. 19, pp. 5491–5505, 2016.

[21] F. Negro, A. Holobar, and D. Farina, "Fluctuations in isometric muscle force can be described by one linear projection of low-frequency components of motor unit discharge rates," *J. Physiol.*, vol. 587, no. 24, pp. 5925–5938, 2009.

[22] A. Holobar and D. Zazula, "Multichannel Blind Source Separation Using Convolution Kernel Compensation," *IEEE Trans. Signal Process.*, vol. 55, no. 9, pp. 4487–4496, Sep. 2007.

[23] A. Holobar, M. A. Minetto, and D. Farina, "Accurate identification of motor unit discharge patterns from high-density surface EMG and validation with a novel signal-based performance metric," *J. Neural Eng.*, vol. 11, no. 1, 2014.

[24] D. Farina and R. Merletti, "A Novel Approach for Precise Simulation of the EMG Signal Detected by Surface Electrodes," vol. 48, no. 6, pp. 637–646, 2001.

[25] T. R. Farrell and R. F. Weir, "The optimal controller delay for myoelectric prostheses," *IEEE Trans. Neural Syst. Rehabil. Eng.*, vol. 15, no. 1, pp. 111–118, 2007.

[26] K. Englehart and B. Hudgins, "A robust, real-time control scheme for multifunction myoelectric control," *IEEE Trans Biomed Eng*, vol. 50, no. 7, pp. 848–854, 2003.

[27] K. C. McGill, Z. C. Lateva, and H. R. Marateb, "EMGLAB: An interactive EMG decomposition program," *J. Neurosci. Methods*, vol. 149, no. 2, pp. 121–133, 2005.

[28] A. M. Castronovo, F. Negro, and D. Farina, "Theoretical Model and Experimental Validation of the estimated proportions of common and independent input to motor neurons," in *2015 37th Annual International Conference of the IEEE Engineering in Medicine and Biology Society (EMBC)*, 2015, pp. 254–257.

[29] J. R. Rosenberg, A. M. Amjad, P. Breeze, D. R. Brillinger, and D. M. Halliday, "The Fourier approach to the identification of functional coupling between neuronal spike trains," *Prog. Biophys. Mol. Biol.*, vol. 53, pp. 1–31, 1989.

[30] S. M. Kay, *Modern Spectral Estimation: Theory and Application*. Prentice Hall, 1999.

[31] Y. Wang, J. Li, and P. Stoica, *Spectral Analysis of Signals: The Missing Data Case*. Morgan & Claypool Publishers, 2006.

[32] M. Teplan, "Fundamentals of EEG Measurement," *Meas. Sci. Rev.*, vol. 2, pp. 59–64, 2002.

[33] D. Farina, R. Merletti, and R. M. Enoka, "The extraction of neural strategies from the surface EMG: an update," *J. Appl. Physiol.*, vol. 117, no. 11, pp. 1215–1230, Dec. 2014.

[34] C. T. Moritz, B. K. Barry, M. A. Pascoe, and R. M. Enoka, "Discharge Rate Variability Influences the Variation in Force Fluctuations Across the Working Range of a Hand Muscle," *J. Neurophysiol.*, vol. 93, no. 5, pp. 2449–2459, 2005.

[35] D. Farina, F. Negro, and J. L. Dideriksen, "The effective neural drive to muscles is the common synaptic input to motor neurons," *J. Physiol.*, vol. 592, no. 16, pp. 3427–3441, Aug. 2014.

[36] C. J. Heckman and R. M. Enoka, "Motor unit," *Compr. Physiol.*, vol. 2, no. 4, pp. 2629–2682, 2012.

[37] D. Farina and F. Negro, "Common Synaptic Input to Motor Neurons , Motor Unit Synchronization , and Force Control," no. 5, pp. 23–33, 2015.

[38] C. K. Thompson *et al.*, "Robust and accurate decoding of motoneuron behaviour and prediction of the resulting force output," *J. Physiol.*, vol. 596, no. 14, pp. 2643–2659, 2018.

[39] C. J. De Luca and Z. Erim, "Common drive of motor units in regulation of muscle force," *Trends Neurosci.*, vol. 17, no. 7, pp. 299–305, 1994.

[40] V. Glaser, A. Holobar, and D. Zazula, "Real-time motor unit identification from high-density surface EMG," *IEEE Trans. Neural Syst. Rehabil. Eng.*, vol. 21, no. 6, pp. 949–958, 2013.